PCCP

Accepted Manuscript

ROYAL SOCIETY OF CHEMISTRY

www.rsc.org/pccp

Synthesis of Poly(ethylene furan-dicarboxylate) polyester using monomers derived from renewable resources. Thermal behavior comparison with PET and PEN

George Z. Papageorgiou, Vasilios Tsanaktsis, Dimitrios N. Bikiaris*

Laboratory of Polymer Chemistry and Technology, Department of Chemistry, Aristotle University of Thessaloniki, GR-541 24, Thessaloniki, Macedonia, Greece

Abstract

Poly(ethylene 2,5-furan dicarboxylate) (PEF) is a new alipharomatic polyester that can be prepared from monomers derived from renewable resources like furfural and hydroxymethylfurfural. For this reason has gained recently high interest. In the present work it was synthesized from the dimethylester of 2,5-furandicarboxylic acid and ethylene glycol by applying the two-stage melt polycondensation method. The thermal behavior of PEF was studied in comparison to its terephthalate and naphthalate homologues poly(ethylene terephthalate) (PET) and poly(ethylene naphthalate) (PEN), which were also synthesized following the same procedure. The equilibrium melting point of PEF was found 265^{o}C while the heat of fusion for the pure crystalline PEF was estimated to be about 137J/g. The crystallization kinetics was analyzed using various models. PET showed faster crystallization rates than PEN and this in turn showed faster crystallization than PEF, under both isothermal and non-isothermal conditions. The spherulitic morphology of PEF during isothermal crystallization was investigated with polarized light microscopy (PLM). Large nucleation density and small spherulites size were observed for PEF even at low supercoolings, in contrast to PET or PEN. Thermogravimetric analysis indicated that PEF is thermally stable till 325^{o}C and the temperature for the maximum degradation rate was 438^{o}C. These values were a little lower than those for PET or PEN.

***Keywords**:* Poly(ethylene 2,5-furan dicarboxylate), furanoate, polyesters, crystallization, multiple melting, thermal degradation.

* Corresponding author. E-mail: dbic@chem.auth.gr

1. Introduction

Nowadays, there is a growing interest in the preparation of new chemicals and materials based on renewable resources, as biomass-derived fuel and chemicals are a promising alternative to fossil based materials. The idea for polymers from renewable resources is not new, however their relatively high cost when compared with their petrochemical homologues was always a major drawback.[1]The current cost of bio-based chemicals used as building blocks is still high, but the situation is expected to change in the near future. The biorefinery concept seems to be answer to the problem. Chemicals from vegetable feedstocks like sugars, vegetable oils, organic acids, glycerol and others have been proposed as monomers for polymer production. In general, biomass-derived monomers can be divided according to their natural molecular biomass origins as: (i) oxygen-rich monomers namely carboxylic acids, polyols, dianhydroalditols, and furans, (ii) hydrocarbon-rich monomers including vegetable oils, fatty acids, terpenes, terpenoids and resin acids, (iii) hydrocarbon monomers such as bio-ethene, bio-propene, bio-isoprene and bio-butene, and (iv) non-hydrocarbon monomers namely carbon dioxide and carbon monoxide.[2]

Aliphatic dicarboxylic acids (ADA) that can be obtained from carbohydrates by the lignocellulosic feedstock biorefinery, including succinic acid, fumaric acid and itaconic acid, are very important monomers. Also, examples of carbohydrate-based aliphatic diols include isosorbide, isomannide and isoidide, 1,3-propanediol and 1,4-butanediol. Suberin and cutin are two other interesting sources of monomers for the preparation of biodegradable polymers. Referring to aromatic monomers, carbohydrates and lignin are the major sources, with 2,5-furandicarboxylic acid (FDCA) and vanillic acid being the most important examples.

ADA and some of these mentioned diols can be used for preparation of polyesters, which consist one of the most important families of plastics with a wide range of applications. Such polyesters appear now as one of the most promising families of polymers based on renewable resources. Some biomass derived polyesters like poly(lactic acid) (PLA), poly(butylene succinate) (PBSu), poly(butylene succinate adipate) (PBSA), etc., are currently among the most promising biodegradable polymers.[3,4] Unfortunately, despite the achievements, these polyesters lack important properties in order to replace completely the conventional plastics that are used extensively today.[5] For this reason there is a demand for new polyesters

prepared from monomers derived from renewable resources, but also having enhanced properties. Such monomers were recently reported that can be synthesized from furfural and hydroxymethylfurfural (HMF), readily available from saccharide sources, simulating those presently prepared from petrol and carbon chemistry.[6] FDCA is one of the most important monomers derived from HMF. Gandini's group has reported synthesis of a series of poly(2,5-furan dicarboxylate)s based on a variety of diols, including ethylene glycol , 1,3-propanediol, 1,4-di(hydroxymethyl)-benzene, hydroquinone, bis(2,5-hydroxymethyl)furan and isosorbide.[7] Synthesis and characterization of bio-based furanic polyesters or copolyesters with ethylene glycol or other diols has been also reported in a few recent works.[8-19]All these polyesters can be used for films, fibers, bottles, thermoforming articles, etc., and are proposed as alternative materials for the already used alipharomatic polyesters (PET, PBT, PEN, PPT, etc.,), since they have comparable properties.

Terephthalate polyesters like PET, poly(butylene terephthalate) (PBT) or poly(propylene terephthalate) (PPT) is a class of high performance thermoplastic polymers with a wide range of applications. However, terephthalate polyesters are resistant to microbial attack and not degradable under normal environmental conditions. Furthermore, their precursors are fossil based. The structure of FDCA is similar to that of terephthalic acid. Novel approaches to the preparation of hydroxymethylfurfural open the way to the large-scale production of FDCA which is used for the production of poly(ethylene-2,5-furandicarboxylate) (PEF).[17]

Another polyester with a lot of similarities with PET is its naphthalate homologue poly(ethylene-2,6-naphthalate) (PEN)[20, 21] which shows comparable or better properties than PET. The improved properties of PEN are a result of the double naphthalene ring. PEN was introduced into the market some years ago, as an alternative material for PET[22], especially for beverage containers since it has enhanced gas barrier properties. However, its cost is much higher than PET.

It was reported that PEF exhibits improved mechanical and barrier properties and for example this could enable light-weighting of beverage packaging.[19] Furthermore, PEF is a material based on renewable resources that could be an alternative for both PET and PEN polyesters and some companies are building pilot plants for the green production of PEF in large scale. However, it is well known that the final properties of polymers depend from their chemical structure and also on the

physical structure of the polymeric materials. PEF is a new polyester and almost all the efforts till today were focus to produce it in high quality and molecular weight. Its physical properties and especially its thermal behavior were not studied in details. For this reason in the present work PEF was synthesized and its thermal and crystallization behavior was studied in comparison with PET and PEN (Scheme 1) in order to assess it as alternative material. As far as we know, the thermal behavior of PEF has not been studied in detail yet.

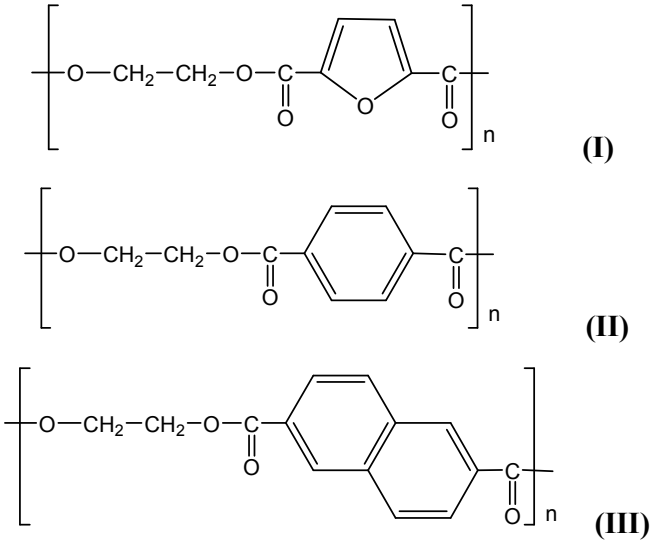

Scheme I. Chemical structures of PEF (I), PET (I) and PEN (III).

2. Experimental

2.1. Materials

Dimethyl-2,6-naphthalate (DMN) was obtained from Amoco Chemicals and Fine Acids Co (purum 99%). Dimethyl terephthalate (DMT) was obtained from Du Pont De Nemours Co and 2,5-furan dicarboxylic acid (purum 97 %) was purchased from Aldrich Co. Ethylene glycol and tetrabutyl titanate (TBT) catalyst of analytical grade were purchased also from Aldrich Co. All other materials and solvents used were of analytical grade.

2.2. Synthesis of 2,5-dimethylfuran-dicarboxylate (DMF)

15.6 g of 2,5-furandicarboxylic acid, 200 mL of methanol anhydrite and 2 mL of concentrated sulfuric acid was transferred into a random flask (500 ml) and the mixture was refluxed for 5 hours. The excess of the methanol was distilled and the

solution was filtered through a disposable Teflon membrane filter. During filtration dimethylester was precipitated as white powder and after cooling 100 mL of distilled water was added. The dispersion was partially neutralized by adding Na_2CO_3 5 % w/v during stirring while pH was measured continuously. The white powder was filtered and the solid was washed several times with distilled water and dried. The isolated white methylester was recrystallized with a mixture of 50/50 v/v methanol/water. After cooling 2,5-dimethylfuran-dicarboxylate (DMF) was precipitated in the form of white needles. The reaction yield was calculated at 83 %.

2.3. Polyester synthesis

The polyesters were prepared by the two-stage melt polycondensation method (esterification and polycondensation) in a glass batch reactor.[5, 23]

For the preparation of PET and PEN the proper amounts of DMT or DMN and EG at a molar ratio of diester/EG=1/2.2 were charged into the reaction tube of the polyesterification apparatus. For the synthesis of PEF higher molar ratio was used (DMF/EG=1/3). TBT (400 ppm) was added as catalyst and the apparatus with the reagents was evacuated several times and filled with argon in order to remove the whole oxygen amount. The reaction mixture was heated at 190^{o}C under argon atmosphere and stirring at a constant speed (350 rpm). For the synthesis of PEF the reagents were first heated at 160^{o}C under argon atmosphere for 2h at 170^{o}C for additional 2 h and finally at 180-190^{o}C for 1h. This first step (transesterification) is considered to complete after the collection of almost all the theoretical amount of CH_3OH, which was removed from the reaction mixture by distillation and collected in a graduate cylinder.

In the second step of polycondensation a vacuum (5.0 Pa) was applied slowly over a period of time of about 30 min to remove the excess of diols and to avoid excessive foaming and furthermore to minimize oligomer sublimation, which is a potential problem during the melt polycondensation. The temperature was gradually increased (1h) for PET and PEN synthesis to 280^{o}C while stirring speed was increased at 720 rpm. The polycondensation continued for about 120 min at 280^{o}C. For PEF synthesis the temperature was slowly increased from 190^{o}C to 220^{o}C while stirring speed was increased at 720 rpm. The reaction continued at this temperature for 2h and after that time the temperature was increased to 235^{o}C for 2h and at 250^{o}C

for additional 2h. After the polycondensation reaction was completed, the polyesters were easily removed, milled and washed with methanol.

2.4. Polyester characterization

2.4.1. Intrinsic viscosity measurement.

Intrinsic viscosity [η] measurements were performed using an Ubbelohde viscometer at 30 ^{o}C in a mixture of phenol/1,1,2,2-tetrachloroethane (60/40, w/w).

Number-average molecular weight (M_n) was measured by Gel permeation chromatography **(**GPC) using a Waters 150^{o}C apparatus equipped with differential refractometer as detector and three ultrastyragel (103, 104, 105Å) columns in series. Hexafluoroisopropanol was used as mobile phase at a flow rate 0.5 mL/min at 40^{o}C. Calibration was performed using polystyrene standards with a narrow molecular weight distribution.

2.4.2. Wide angle X-Ray diffraction patterns (WAXD).

X-ray diffraction measurements of the samples were performed using a MiniFlex II XRD system from Rigaku Co, with CuK_{α} radiation (λ=0.154 nm) in the angle 2θ range from 5 to 60 degrees.

2.4.3. Differential Scanning Calorimetry (DSC).

A Perkin–Elmer, Pyris Diamond DSC differential scanning calorimeter, calibrated with pure Indium and Zinc standards, was used. The system also included an Intracooler 2P cooling accessory, in order the DSC apparatus to achieve function at sub-ambient temperatures and high cooling rates. Samples of 5±0.1 mg sealed in aluminium pans were used, to test the thermal behavior of the quenched polymers. The samples were cooled to 50^{o}C and then heated at a rate 20°C/min to above the melting temperature. In order to obtain amorphous materials, the samples were heated to 40 ^{o}C above the melting temperature and held there for 5 min, in order to erase any thermal history, before cooling in the DSC with the highest achievable rate.

Isothermal crystallization experiments of the polymers at various temperatures below the melting point were performed after self-nucleation of the polyester sample. Self-nucleation measurements were performed in analogy to the procedure described by Fillon et al.[24] The protocol used is very similar with that described by Müller et

al.[25] and can be summarized as follows: a) melting of the sample at 40 ^{o}C above the observed melting point for 5 min to erase any previous thermal history; b) cooling at 10 ^{o}Cmin^{-1} to a reference temperature and crystallization, to create a ''standard'' thermal history; c) partial melting by heating at 20 ^{o}Cmin^{-1} up to a ''self-nucleation temperature'', T_s which differed for the various polymers ; d) thermal conditioning at T_s for 5 min. Depending on T_s, the crystalline polyester will be completely molten, only self-nucleated or self-nucleated and annealed. If T_s is sufficiently high, no self-nuclei or crystal fragments can remain (T_s Domain I - complete melting domain). At intermediate T_s values, the sample is almost completely molten, but some small crystal fragments or crystal memory effects remain, which can act as self-nuclei during a subsequent cooling from T_s, (T_s Domain II-self - nucleation domain). Finally, if T_s is too low, the crystals will only be partially molten, and the remaining crystals will undergo annealing during the 5 min at T_s, while the molten crystals will be self-nucleated during the later cooling, (T_s Domain III - self-nucleation and annealing domain); e) cooling scan from T_s at 200 ^{o}Cmin^{-1} to the crystallization temperature (T_c), where the effects of the previous thermal treatment will be reflected on isothermal crystallization; f) heating scan at 20 ^{o}Cmin^{-1} to 40^{o}C above the melting point, where the effects of the thermal history will be apparent on the melting signal. Experiments were performed to check that the sample did not crystallize during the cooling to T_c and that a full crystallization exothermic peak was recorded at T_c. In heating scans after isothermal crystallization the standard heating rate was 20^{o}C/min.

To investigate the non-isothermal crystallization of the polymers from the melt, the same melting procedure as described above for the isothermal crystallization was followed and then the samples were cooled from the melt at different cooling rates ranging from 2.5 to 20^{o}C/min.

Data obtained were treated using various kinetic models.[26]

2.4.4. Polarizing Light microscopy (PLM)

A polarizing light microscope (Nikon, Optiphot-2) equipped with a Linkam THMS 600 heating stage, a Linkam TP 91 control unit and also a Jenoptic ProgRes C10Plus camera with the Capture Pro 2.1 software was used for PLM observations.

2.4.5. Thermogravimetric analysis (TGA)

Thermogravimetric analysis was carried out with a SETARAM SETSYS TG-DTA 16/18 instrument. Samples (5.0 ± 0.3 mg) were placed in alumina crucibles. An empty alumina crucible was used as reference. Polyesters were heated from ambient temperature to 550 °C in a 50 mL/min flow of N_2 at heating rate of 10 °C/min. Continuous recordings of sample temperature, sample weight and heat flow were taken.

3. Results and discussion

3.1. Characterization of synthesized polyesters

PEF, PET and PEN polyester samples were synthesized by applying the two step polycondensation method as was described in detail in the experimental section. The intrinsic viscosity values were 0.45 dL/g for PEF, 0.43 dL/g for PEN samples and 0.47 dL/g for PET. This indicates that polyesters with similar molecular weights have been prepared, which was also proved from GPC analysis. The differences in the number average molecular weight (Mn) of the studied polyesters are not higher than 2500 g/mol, with PET to have the highest molecular weight (Mn=13700 g/mol), PEF has Mn=11200g/mol and PEN 12100 g/mol (please see Fig. S1 of supplementary material). Thus any recorded difference in crystallization behavior should be attributed to their chemical structure alone.

The WAXD patterns of semicrystalline PEF, PET (α-type crystals) and PEN (α-type crystals) are compared in Fig. 1. PEN showed characteristic peaks at 2θ 11.4 corresponding to (001), 15.5° for the (010) plane, 19.5°, 20.3 ° for the $(\bar{1}03)$, 23.3° for the (100) and 26.8° corresponding to the $(\bar{1}00)$ plane. PET showed its characteristic reflections at 16.5°, 17.7° for (010) plane, 21.6°, 22.7° for the $(\bar{1}00)$ plane and 26.1° (corresponding to the (110) plane) and at 32.9 for the $(0\bar{2}1)$ plane. In the pattern of PEF peaks appeared at 9.1°, 15.1°, 16.9°, 19.7°, 22.4° and 25.5°. The pattern of PEF is the same with that reported Gandini et al.[8] Unfortunately, data about the unit cell of PEF have not been reported yet. As one can see, the pattern of PEF shows some similarity with that of PET. Due to the similarity in the chemical structures and the repeating units of PET and PEF, similarity is also expected in the repeating unit in the crystalline structure and thus in the unit cell parameters of PET and PEF. Similarity was also found between the crystal unit cells of PBT and PBF BY Gazzano et al.[13]

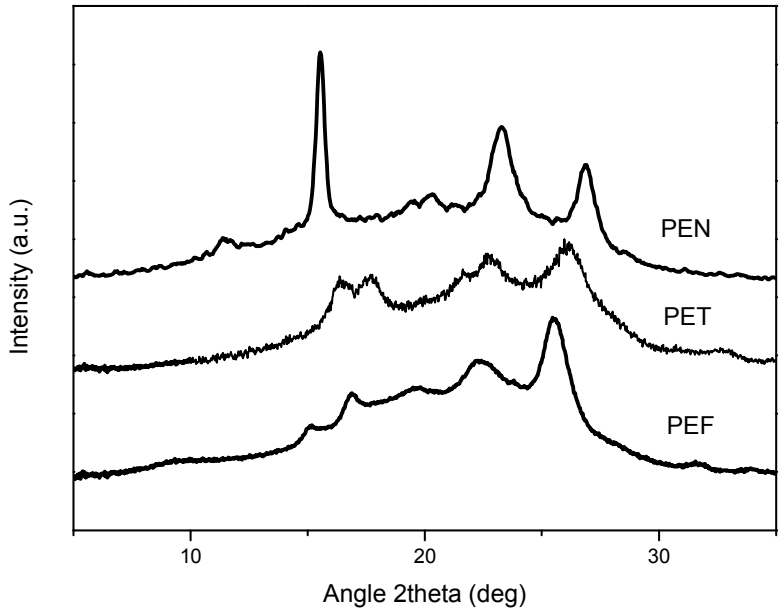

Fig. 1. WAXD patterns of semicrystalline PEF, PET (α- type crystals) and PEN (α-type crystals).

The thermal behavior of the semicrystalline polyesters was studied by using DSC. Fig. 2a shows the DSC traces for the as received and the melt-quenched PEF samples. The former was semicrystalline, as was already proved from WAXD, since some crystallinity formed during the slow cooling in the glass reactor used for the polyester synthesis. The heat of fusion of this sample was found to be about 41J/g. The quenched sample was taken almost completely amorphous and during heating it showed a glass transition temperature of 87^{o}C and a cold crystallization peak at 185^{o}C. The melting point of PEF as measured from the heating scan of the as received sample was 220.7^{o}C. In comparison, the melting points for PET and PEN were found to be 253^{o}C and 271^{o}C respectively.

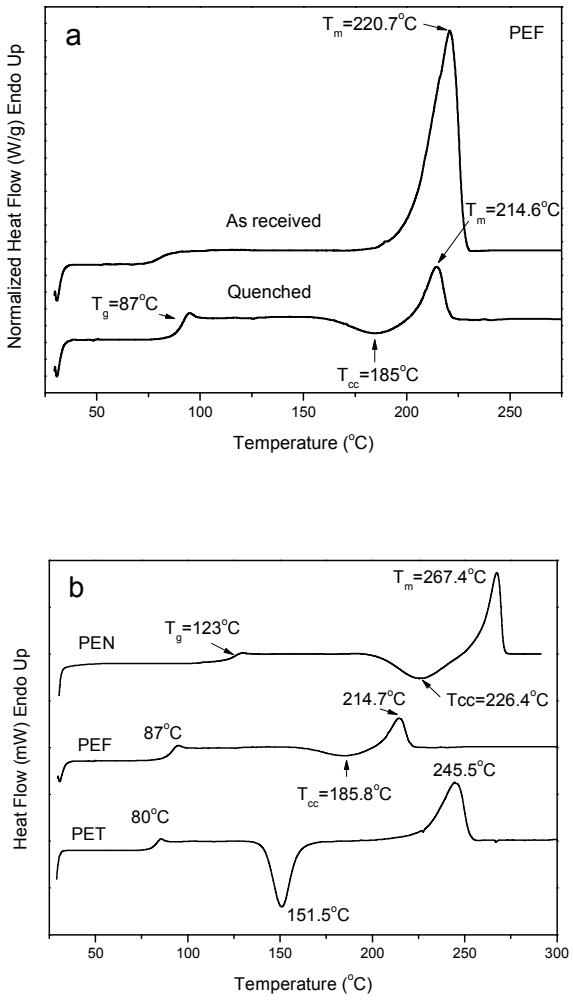

Fig. 2. DSC traces for a) as received and melt-quenched PEF and b) melt-quenched PET, PEF and PEN samples.

Fig. 2b shows the heating scans at 20°C/min for the quenched polyester samples. The glass transition temperatures (T_g) of the polymers increase from that for PET (T_g=80°C) to that for PEF (T_g=87°C) and finally to the value (T_g=123°C) for PEN. The increase in the heat capacity was ΔC_p = 0.460 $Jg^{-1}K^{-1}$ for PEF, which is higher than the reported for PET[27]that is 0.405 $Jg^{-1}K^{-1}$ and also higher than that for PEN (0.38 $Jg^{-1}K^{-1}$).[28] For these melt quenched samples the measured melting points were 214.7°C, 245.5°C and 267.4°C for PEF, PET and PEN respectively, which are lower than the corresponding of semicrystalline samples. This means that PEF shows higher T_g but lower T_m compared to PET. As one can also see in Fig. 2b, PET shows a

sharp cold-crystallization peak at T_{cc}=151°C, about midway from T_g and T_m while for PEF and PEN the cold crystallization peak appears close to the melting peak, at T_{cc}=185.8°C for PEF and at T_{cc}=226.4°C for PEN. Furthermore, the crystallization peak is broad and shallow for PEF.

3.2. Multiple melting behaviors

The melting behaviors of the polyesters after isothermal crystallization from the melt were investigated with DSC. As can be seen in Fig. 3 PEF samples, PET and PEN, showed multiple melting. In fact three melting peaks can be observed in the respective DSC heating traces of PEF after isothermal crystallization from the melt (Fig. 3a). In the heating traces corresponding to samples crystallized at high temperatures (T_cs), the melting peaks coincided. In general, a very small peak (peak I) appeared just after the crystallization temperature (4-5°C above T_c) and it is the well known annealing peak which is usually attributed to the melting of the secondary crystals. The middle temperature peak (peak II) increased in both temperature and heat of fusion with increasing crystallization temperature, so it should be attributed to the melting of the original crystals formed during the isothermal crystallization stage. Finally, the ultimate melting peak (peak III) increased in temperature with increasing the crystallization temperature. The multiple melting behavior of PEF is rather consistent with the two populations of lamellae of different stabilities rather than recrystallization. WAXD study of samples crystallized at different temperatures, in the temperature range from 150 to 200°C, gave similar patterns where the same peaks are always present, although the peaks for samples crystallized at high temperatures were sharper (Figure 3b). This indicated that the multiple melting behavior and the differences in the melting behaviors of samples crystallized at different temperatures are not associated with melting of crystals of different forms created during the isothermal crystallization stage. Furthermore, WAXD patterns of samples initially crystallized at 180°C or 200°C were compared with those after further annealing at higher temperatures. In all the patterns the same peaks were observed. However, the peaks became sharper after further annealing of the samples showing more perfect crystals and narrower crystal size distributions. These observations proved that there was no crystal transition to a different crystal modification upon heating.

The multiple melting behaviors of PET and PEN can be seen in Fig. 2c and 2d, respectively. In general, like for PEF the multiplicity of the melting peaks depended on the crystallization temperature. In case of PET and for low crystallization temperatures even a fourfold melting was observed, although the annealing peak was very weak. PEN on the other hand showed a clear triple melting. The partial melting-recrystallization-final melting scheme is well accepted for the interpretation of PET and PEN too. In every case, crystallization at high T_cs was slow and required long time, but it also resulted in high melting points due to crystal thickening.

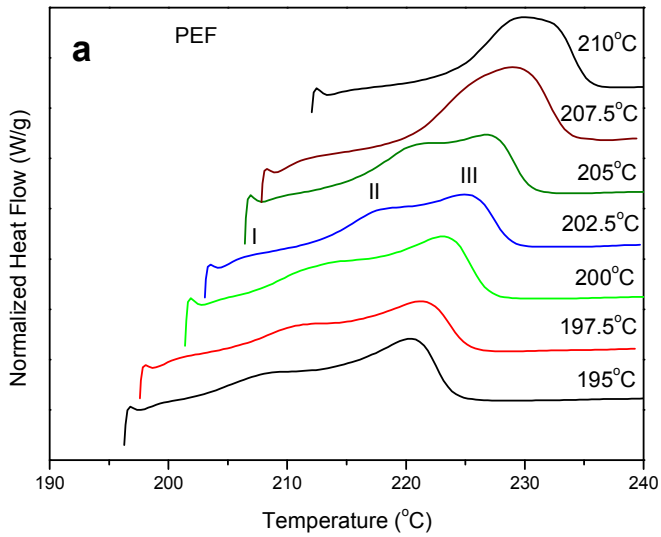

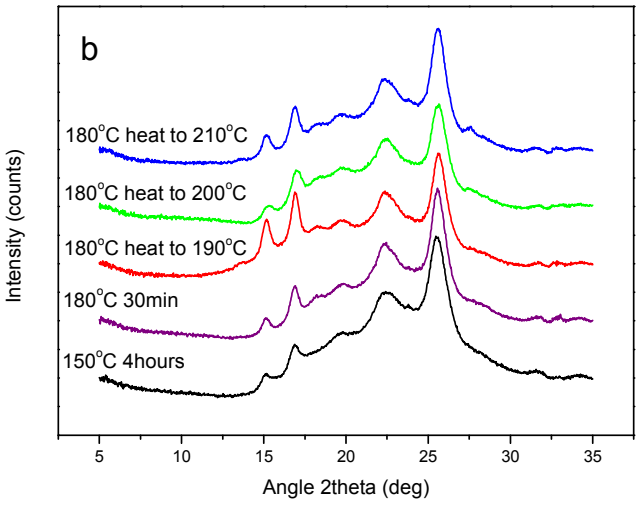

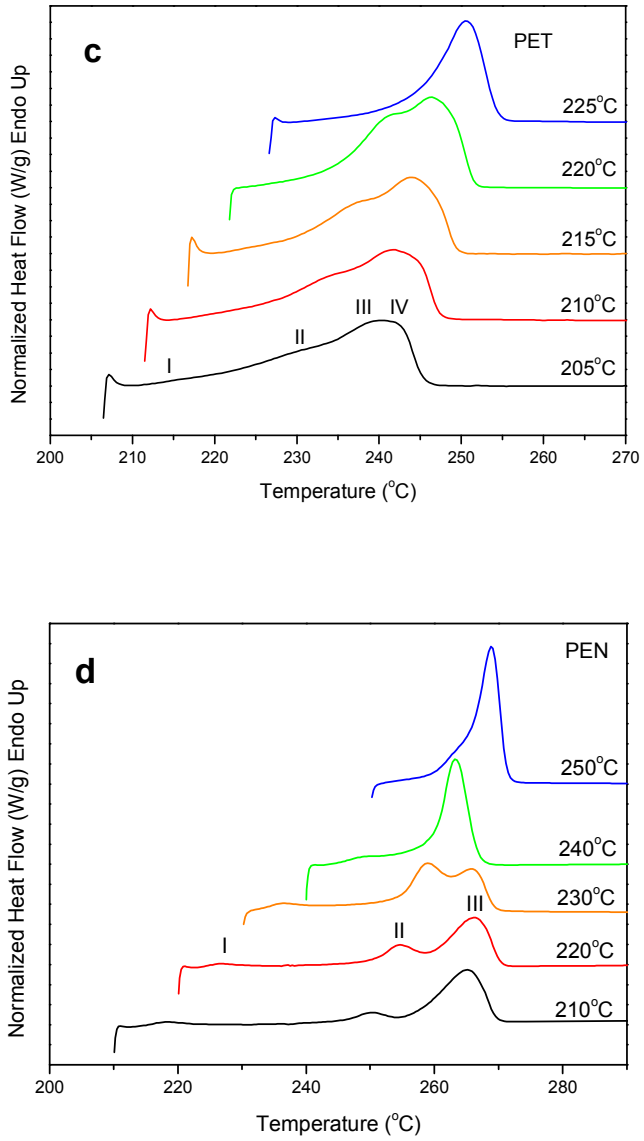

Fig. 3. DSC heating scans after isothermal crystallization at the indicated temperatures for a) PEF, b) PET and c) PEN.

Like for the polyesters of this work, multiple melting is often observed in DSC traces of thermoplastics after isothermal crystallization[29-30] and have been attributed to the melting of crystals of different stability (dual morphology mechanism) and the melting, re-crystallization, re-melting process (reorganization mechanism).[31] The dual morphology mechanism assumes formation during the isothermal crystallization, before DSC heating scan, of two or more different crystalline structures in the

crystallized polymers i.e. (a) two or more crystal modifications, (b) at least two populations of lamellae of different stabilities or (c) different crystalline morphologies.[31] Since melting of the originally formed crystals exclusively is very difficult to be observed, for polymers the origin of the multiple melting peaks appearing in differential scanning calorimetry (DSC) curves is still controversially discussed. Recent works utilizing fast chip calorimetry allow better understanding of melting. [32, 33]

3.3. Equilibrium melting Point using the Hoffman-Weeks method

The equilibrium melting temperature (T_m^o) of a polymer is usually estimated using the Hoffman-Weeks extrapolation [34]. In this procedure, the measured T_ms of specimens crystallized at different crystallization temperatures (T_cs) are plotted against T_c and a linear extrapolation to the line T_m=T_c, and the intercept gives T_m^o. In the Hoffman-Weeks equation:[34]

$$T_m = T_m^o\left(1-\frac{1}{2\beta}\right)+\frac{T_c}{2\beta} \qquad (1)$$

T_m is the observed melting temperature of a crystal formed at a temperature T_c, β is the thickening equal to L_c/L_c^* β indicates the ratio of the thickness of the mature crystallites L_c to that of the initial ones L_c^* .[34] The prerequisite for the application of this theory is the isothermal thickening process of lamellar crystals at a specific crystallization temperature and the dependence of the thickening coefficient on the crystallization temperature. Fig. 4a shows the Hoffman-Weeks plot for PEF. The ultimate peak temperature values were used and a value of T_m^o=265°C was found which is much lower than the corresponding of PET (T_m^o=294°C)[35] and PEN (T_m^o=337°C). [21, 28] In fact, the middle peak temperatures were also used in order to estimate the T_m^o of PEF. However, in this case the slope of the plot was larger than 1, which is unacceptable.

3.4. Enthalpy of fusion of the pure crystalline PEF

The heat of fusion of the pure crystalline polymer is a very important parameter which can be used for the estimation of the degree of crystallinity of polymer specimens. Prior to determine ΔH_m^o of PEF a series of samples with different degrees of crystallinity was prepared and WAXD patterns of the samples and the corresponding

DSC traces on heating were recorded (Fig. S2). To prepare the samples with the different crystallinity values an originally amorphous PEF sample was heated for different times at 150°C. From the DSC traces the heat of fusion of these samples was measured. The crystallinity values were calculated from the WAXD patterns and the relative areas under the crystalline peaks, A_c, and the amorphous background, A_{am}, using the following equation:

$$X_c = (1 + A_{am} / A_c)^{-1} \quad (2)$$

according to Hay et al. [36]

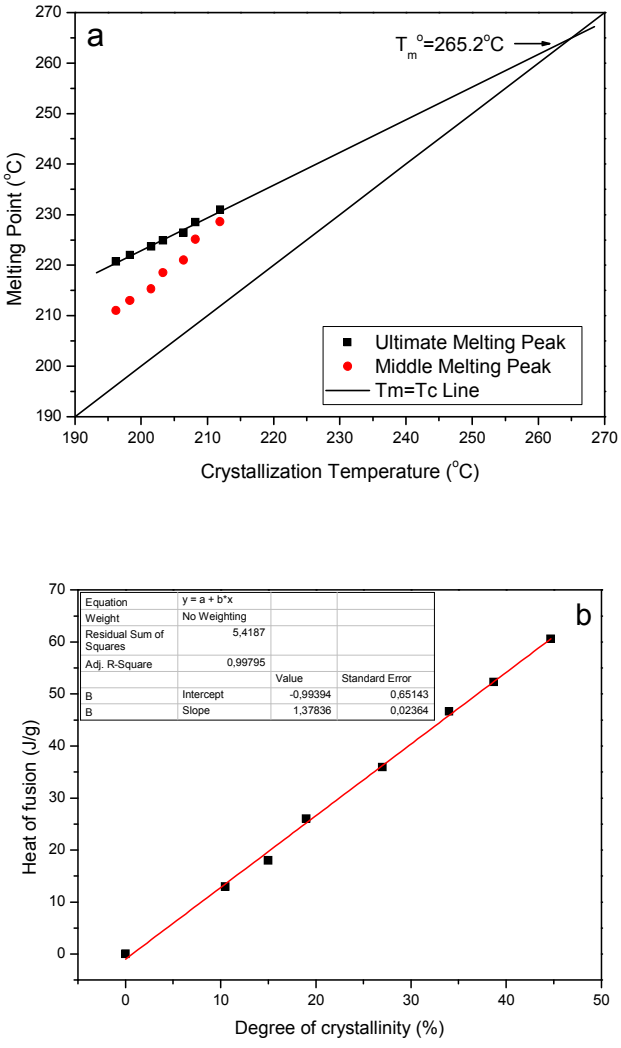

Fig. 4. a) Hoffman-Weeks plot for the estimation of the equilibrium melting point of PEF and b) plot of the measured heat of fusion against the degree of crystallinity calculated from WAXD patterns.

The plot of the heat of fusion that measured with DSC as a function of the degree of crystallinity was constructed (Figure 4b) and with extrapolation to 100% crystallinity the value of ΔH_m^o=137J/g was found. This value is close to that for PET (ΔH_m^o= 140J/g) but higher than that for PEN (ΔH_m^o= 103J/g).[37]

3.5. Isothermal crystallization from the melt

The isothermal crystallization kinetics of PEF after self-seeding was studied with DSC at temperatures from 165 to 205°C (Fig. S3). The procedure was described in the experimental part. The exothermal curves were recorded as a function of crystallization time which kept becoming longer along with the broadening of the exothermic peaks with increasing T_c. The development of relative crystallinity with crystallization time for the studied samples at different temperatures was obtained since the assumption that the evolution of crystallinity is linearly proportional to the evolution of heat released during the crystallization was made:

$$X(t) = \frac{\int_0^t (dH_c / dt)dt}{\int_0^\infty (dH_c / dt)dt} \quad (3)$$

where dH_c denotes the measured enthalpy of crystallization during an infinitesimal time interval dt. The limits t and ∞ on the integrals are used to denote the elapsed time during the course of crystallization and at the end of the crystallization process, respectively. Fig. 5a shows the development of relative crystallinity with crystallization time at different temperatures for PEF. It can be seen that the typical sigmoidal curves were obtained and the crystallization time prolongs with increasing crystallization temperature, suggesting that the crystallization is slowed down at high T_c. As can be seen from Fig. 5a the crystallization rate of PEF is very high at temperatures 165-185°C and the time for complete crystallization is short. Isothermal crystallization of PET and PEN was also investigated. Crystallization temperatures ranged from 180 to 210°C for PET and from 210 to 245°C for PEN samples. From the plots of the relative degree of crystallinity with time, the half time of crystallization $t_{1/2}$, which represents the time needed for a particular sample to achieve 50% of the

total crystallinity which the material is capable of developing during the isothermal crystallization process, was determined.

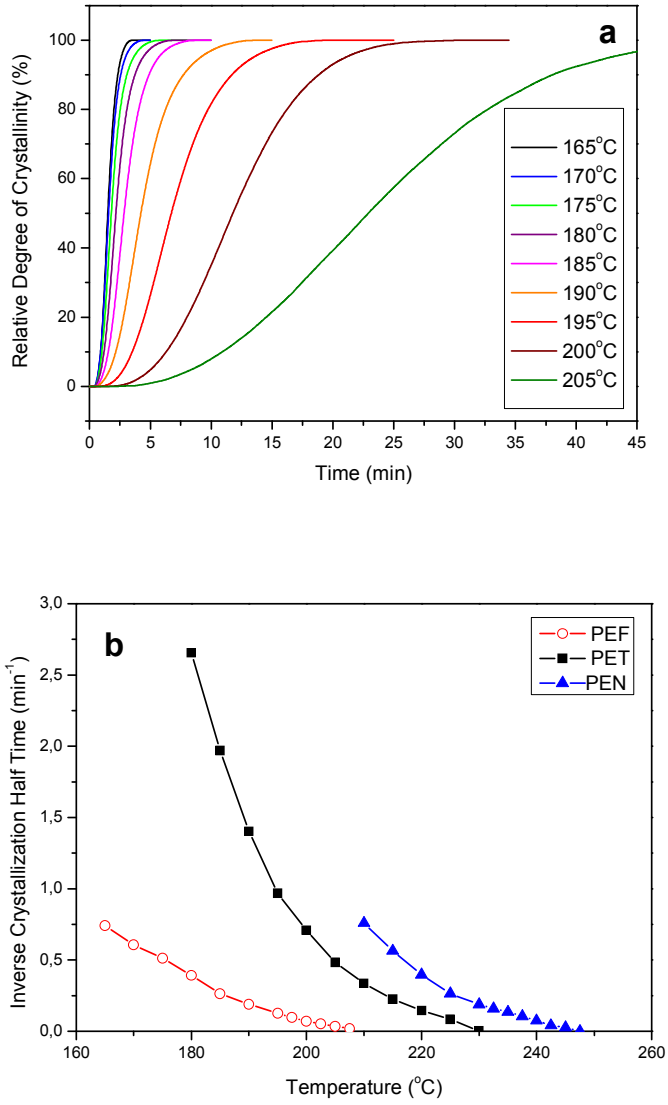

Fig. 5. a) Evolution of Relative Degree of Crystallinity with time during isothermal crystallization of PEF at different temperatures and b) inverse Isothermal Crystallization Half-Time as a function of crystallization temperature.

The inverse crystallization half-time is often used as a measure of the overall crystallization rate. Fig. 5b shows the plots of the inverse crystallization half-time with crystallization temperature for all the polyesters. As can be seen, the crystallization rates decrease with increasing crystallization temperature. However,

the temperature ranges are different for the studied polyesters. PET shows high crystallization rates in the temperature range 180-200°C while PEN shows high rates at 210-225°C, which are much higher than the corresponding of PEF (165-185°C). The driving force for crystallization is the supercooling, that is the difference between the melting point and the crystallization temperature ($\Delta T=T_m-T_c$). So, it is interesting to compare the crystallization rates at given supercooling. From the corresponding plots (Fig. S4) it was proved that PET has faster crystallization rates than PEN and this in turn shows faster crystallization than PEF at given supercooling.

For the analysis of the isothermal crystallization, the most common approach is the so-called Avrami method.[38] Accordingly, the relative degree of crystallinity, *X(t)*, is related to the crystallization time, *t*, according to:

$$X(t) = 1 - \exp(-kt^n) \qquad or \qquad X(t) = 1 - \exp[-(Kt)^n] \tag{4}$$

where, *n* is the Avrami exponent which is a function of the nucleation process and *k* is the growth function, which is dependent on nucleation and crystal growth. Since the units of *k* are a function of *n*, equation (4) can be written in the composite–Avrami form using *K* instead of *k* (where $k = K^n$).[39]

The values of *n*, *k* and *K*, can be calculated from fitting to experimental data using the double logarithmic form of equation (4):

$$\log\{-\ln[1 - X(t)]\} = \log k + n \log t \tag{5}$$

Equation (4) is thus used to fit the experimental data for PEF. Plots of $\log\{-\ln[1 - X(t)]\}$ vs $\log t$ were constructed and are shown in Fig. 6a.

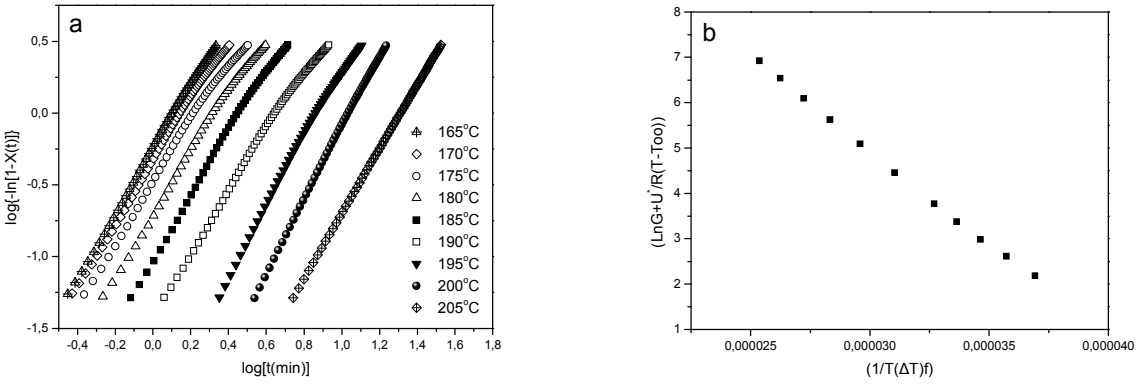

Fig. 6. a) Avrami plots for the isothermal crystallization and b) Lauritzen-Hoffman plot for PEF.

In these plots an initial linear part is observed, which was used for the estimation of the parameters *n* and *k*. The deviation, which is observed after this first linear part in the Avrami plots, is often attributed to secondary crystallization. From the slope and the intersection of the Avrami plots, values of *n* and *k,* respectively, were calculated and the results are summarized in Table 1. In the same table, the values of *K* calculated from the respective values of *n* and *k*, are included. It is known that the value of *n* strongly depends on both the mechanism of nucleation and the morphology of crystal growth, and that ideally *n* would be an integer. [38] As a matter of fact the Avrami constant values ranged from 2.17 to 2.58. A slight increase is apparent with increasing crystallization temperature. These values compare well with those for PET or PEN. [40, 21]

Table 1 Results of the Avrami analysis for the isothermal crystallization of PEF.

Crystallization Temperature (^{o}C)	Avrami exponent n	Avrami constant k	Avrami constant K
165	2.32	0.57815	0.78940
170	2.25	0.47311	0.71624
175	2.21	0.33334	0.60768
180	2.24	0.19466	0.48096
185	2.30	0.09258	0.35491
190	2.17	0.03888	0.22330
195	2.58	0.00653	0.14218
200	2.58	0.00215	0.09276
205	2.25	0.00111	0.04891

3.6. Application of secondary nucleation theory

It has been suggested that the kinetic data of isothermal polymer crystallization can be analyzed using the spherulitic growth rate in the context of the Lauritzen-Hoffman secondary nucleation theory. [41] The theory predicts that the crystallization rate (G(T)) can be expressed as a function of supercooling ΔT according to the expression: [41]

$$G = G_0 \exp\left[-\frac{U^*}{R(T_c - T_\infty)}\right] \exp\left[-\frac{K_g}{T_c(\Delta T) f}\right] \quad (6)$$

where G_0 is the pre-exponential factor and the first exponential term contains the contribution of diffusion process to the growth rate, where U* is the activation energy for the transport of the chains to the growing front (a value of 1500 cal/mol is usually

employed), R is the universal gas constant, T_∞ is the temperature below which diffusion stops, usually set to $T_\infty=T_g-30K$.[41] K_g is the nucleation parameter and ΔT denotes the degree of undercooling ($\Delta T=T_m^0-T_c$), f is a correction factor which is close to unity at high temperatures and is given as $f=2T_c/(T_m^0+T_c)$. The equilibrium melting point of PEF was set 265°C.

The parameter K_g contains the variable n reflecting the regime behavior and it can be expressed as: [41]

$$K_g = \frac{jb_0\sigma\sigma_e T_m^0}{k_B(\Delta h_f)} \quad (7)$$

where j=4 for regimes I and III and j=2 for regime II. b_0 is the thickness of a single stem on the crystal, σ is the lateral surface free energy, Δh_f is the enthalpy of fusion and k_B is Boltzmann's constant. It has been stated that the inverse of the crystallization half times as obtained from DSC isothermal crystallization experiments can be used in place of the spherulite growth rate. [42, 43] Furthermore, the inverse of the crystallization half times after self-nucleation lead to more correct values. [25]

The nucleation constant K_g is calculated from the double logarithmic transformation of Eq. 6:

$$\ln(G)+\frac{U^*}{R(T_c-T_\infty)}=\ln(G_0)-\frac{K_g}{T_c(\Delta T)f} \quad (8)$$

Plotting the left hand side of Eq. 8 (where $G\approx 1/t_{1/2}$) versus $1/T_c(\Delta T)f$ a straight line should occur whose slope and intercept will be equal to $-K_g$ and G_0 respectively (Fig. 6b). For the crystallization temperatures studied it was assumed that regime III holds, given the high nucleation rate of PEF at these temperature as will be discussed in the section for PLM observations. Results showed a $K_{gIII}=4.1\text{x}10^5$ for PEF. In previous works for PET it was found that in regime $K_{gII}=2.5\ \text{x}10^5$ or $K_{gII}=2.2\ \text{x}10^5$. [36, 40] According to the theory $K_{gIII}=2K_{Gii}$ thus a value of $K_{gIII}=4.4\ \text{x}10^5$ to $5\text{x}10^5$ is calculated for PET. However, this value is much lower than that for PEN ($K_{gIII}=8.4\text{x}10^5$).[21]

3.7. Non-isothermal Cold crystallization

Non-isothermal cold-crystallization experiments at various heating rates were performed for melt-quenched samples of the polyesters. Fig. 7a shows the heating scans of PEF samples. As can be seen the cold-crystallization peak shifted to the higher temperature range with increasing heating rate. Furthermore, the melting points of the samples heated at slower rates were higher. This was due to the increased crystal stability, which is finally achieved via the crystal perfection processes occurring after crystal formation and before final melting. Crystal perfection is favored by slow heating rates, as enough time is offered. In case of faster rates, e.g. 20°C/min, the cold crystallization peak appeared just before the melting, so the temperature interval between crystallization and melting is too small and also because of the fast heating rate, the time available for reorganization of the crystals before final melting is very short.

The case was different for PET (Fig. 7b). The cold crystallization peak always appeared at about the middle of the range between glass transition and melting. Thus, recrystallization or reorganization occurred in all cases and the melting point was less affected by the heating rate. The heat of fusion was also not significantly affected. PEN showed a behavior rather similar to PEF, although the crystallization rates seemed to be a little faster (Fig. 7c).

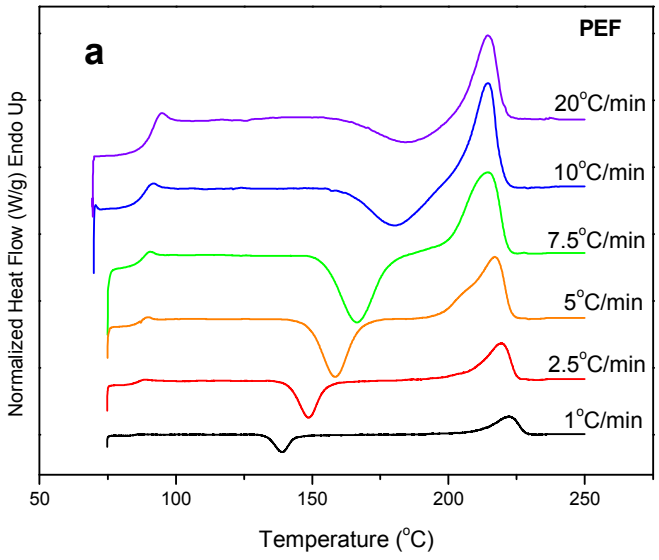

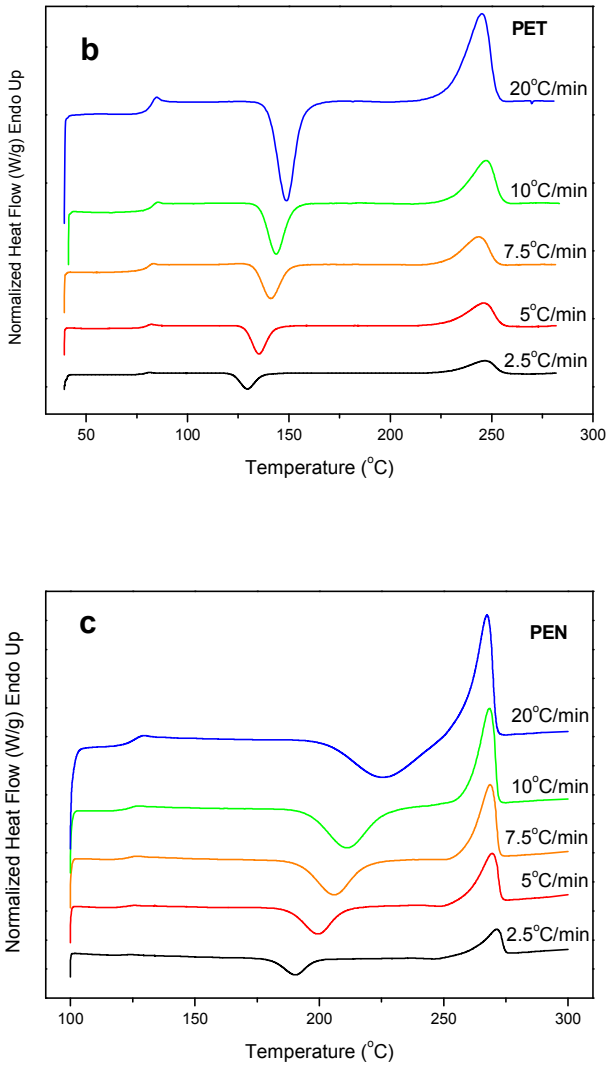

Fig. 7. DSC scans at different heating rates for melt quenched a) PEF, b) PET and c) PEN samples.

To evaluate the cold-crystallization rates of the three polyesters the peak temperature was plotted against heating rate, as can be seen in Fig. 8a while Fig. 8b shows the temperature distance between cold-crystallization temperature and the glass transition temperature. It is apparent in this figure that PET crystallized closer to the T_g than the other two polymers. PEF showed also a slightly smaller difference T_{cc}-T_g than PEN. This shows that the PEF macromolecular chains are more flexible than those of PEN. Also, symmetry is a key factor for crystallizability. At this point it

should be noted that PET repeating unit is more symmetric than that of PEN, while the repeating unit of PEN is, in its turn, more symmetric than that of PEF.

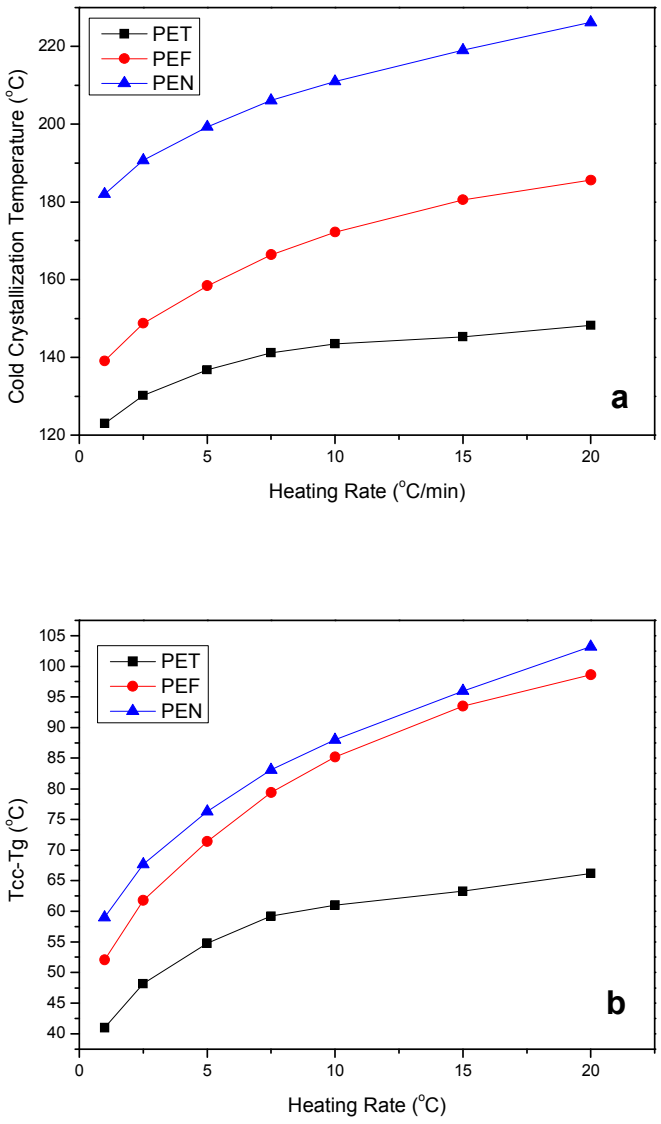

Fig. 8. a) Cold crystallization peak temperature as a function of the heating rate for melt quenched PET, PEF and PEN samples and b) temperature difference T_{cc}-T_g for the polyesters.

To investigate details of the thermal behavior of the quenched samples of the polyesters Step Scan DSC experiments were performed. Step-Scan DSC introduces true isothermal steps between heating steps and its signal attributes different

contributions during the heating procedure of semicrystalline polymers.[44] Crystallization endotherms only contribute to the non-reversing signal, thus separation of exotherms from reversing melting or other heat capacity events is achieved. Unfortunately, exothermic and endothermic non-reversible events can occur simultaneously and they cannot be completely separated from each other. [45, 46] Thus, TMDSC techniques can separate crystallization and recrystallization exotherms, from glass transition, reversible melting or other heat capacity events.

Fig. 9 shows the total, reversing and non-reversing signals for the three polyesters. In every case, in the non-reversing signal curves recrystallization exothermic peaks follow the cold-crystallization ones. For PEF (Fig. 9a) the recrystallization was continuous and began just after the end of cold-crystallization. Non-reversing melting was not obvious. In contrast, for PET recrystallization started 25°C above the end of recrystallization and it showed its maximum rates in the melting region (Fig. 9b). A small non-reversing melting peak was apparent, that is an endothermic peak after recrystallization in the non reversing signal curve of PET. Finally, in the non-revering signal curve for PEN (Fig. 9c) significant amount of recrystallization was observed, but only at high temperatures and the respective peak was narrow compared to that for PEF or even PET.

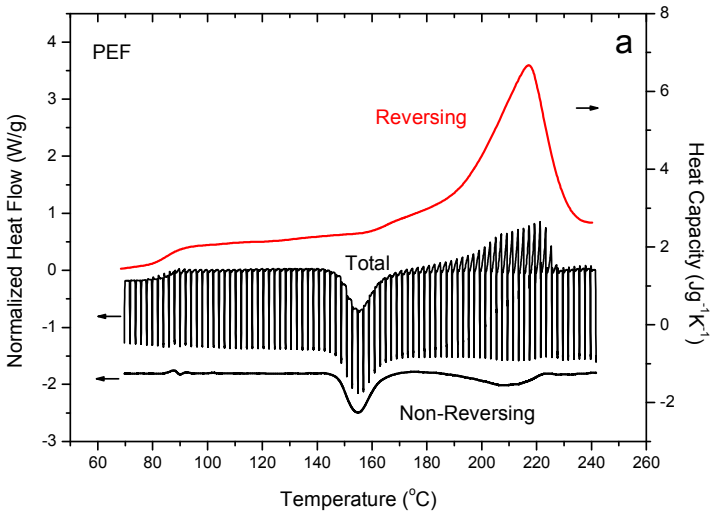

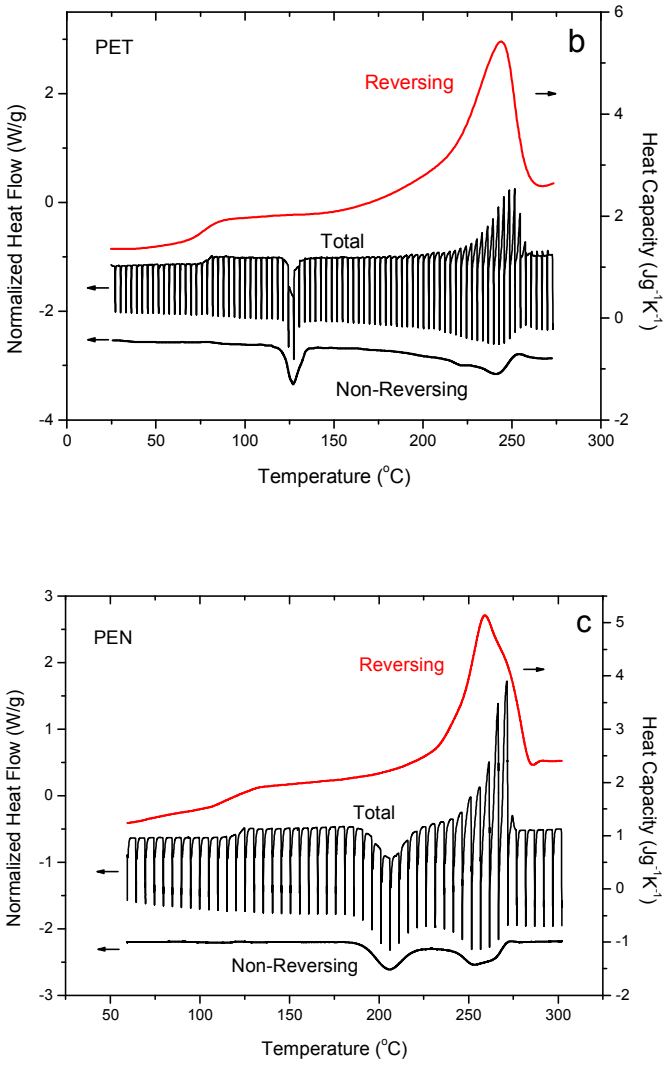

Fig. 9. Step Scan DSC results for a) PEF, b) PET and c) PEN.

3.8. Non-isothermal melt crystallization

The nonisothermal crystallization on cooling from the melt is a process with practical applications in polymer processing. So, the crystallization on cooling at various rates from the melt was studied for the three polyesters. The respective DSC traces on cooling at rates ranging from 2.5 to 20^{o}C/min for PEF can be seen in Fig. 10a. As one can see with increasing cooling rate the exothermic crystallization peak shifted downwards to lower temperatures. Fig. 10b shows the variation of the crystallization peak temperature with increasing cooling rate for the three polyesters. It is obvious that PEN crystallized at the highest temperatures, while PEF at the lowest, following

the order of the melting points. Furthermore, it is important to calculate the supecooling needed for crystallization for the various cooling rates. The plots of the respective supercooling vs cooling rate (Fig. S5) showed that PEF needed the highest supercoolings to crystallize, with an exception for the slower rates where its supercoolings were slightly smaller than those for PEN.

The crystallization temperature T_c, can be converted to crystallization time, t, with the well-known relationship for non-isothermal crystallization processes that is strictly valid when the sample experiences the same thermal history as designed by the DSC furnace: [47]

$$t = \frac{(T_o - T_c)}{a} \tag{11}$$

where a is the constant cooling rate, T_o is the temperature at the beginning of crystallization and T_c is the crystallization temperature at time t. So, the experimental data for degree of crystallinity as function of temperature obtained from the DSC cooling scans were transformed to data as a function of time.

The Avrami equation has been modified to analyze the non-isothermal kinetics on cooling. [47, 48] According to the modified Avrami method, the relative degree of crystallinity, X, can be calculated from:

$$X = 1 - \exp\left(-Z_t t^n\right) \quad or \quad X = 1 - \exp\left[-(K_{Avrami} t)^n\right] \tag{12}$$

where Z_t and n denote the growth rate constant and the Avrami exponent, respectively. Since the units of Z_t are a function of n, equation (12) can be written in the composite–Avrami form using K_{Avrami} instead of Z_t (where $Z_t = K_{Avrami}^n$).

Again Z_t and n can be calculated by fitting the experimental data to an equation similar to equation (4). In Fig. 10c plots of $\log\{-\ln(1-X)\}$ versus $\log(t)$ are shown for PEF. As it can be seen straight lines (till a high value of degree of relative crystallinity) were obtained in each cooling rate and from the slope and intercept of the linear part of each line n and $\log(k)$ are calculated and the best fitting values for the parameters n, Z_t and K_{Avrami} are presented in Table 2. As one can see the Avrami exponent n values decreased with increasing cooling rate, while the Avrami constant values increased. The k or K values are indicative of the crystallization rate. [46] The increase in the crystallization rate is plausible. With increasing the cooling rate, the crystallization temperature decreases, so the supercooling increases and crystallization rate increases.

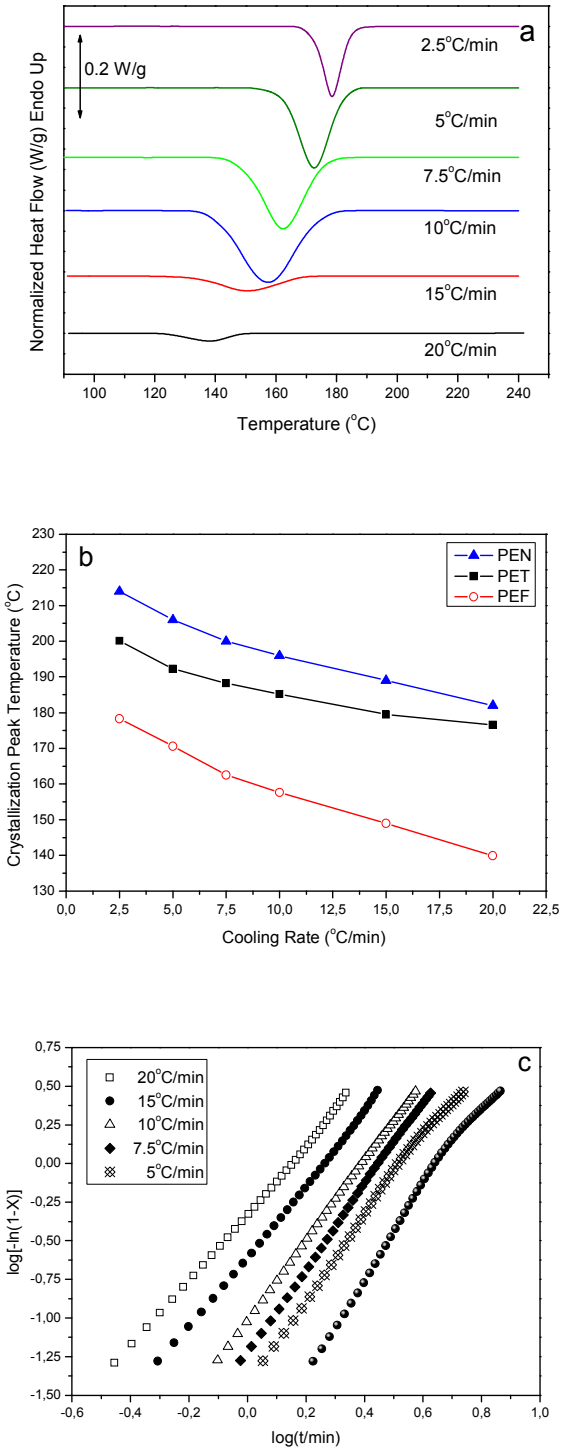

Fig. 10. a) DSC traces on cooling from the melt at different rates for PEF, b) crystallization peak temperature as a function of the cooling rate and c) Avrami plots for the non-isothermal crystallization of PEF on cooling.

Table 2. Results of the Avrami analysis of non-isothermal crystallization of PEF on cooling from the melt.

Cooling Rate (°C/min)	Avrami exponent n	Avrami constant Z_t	Avrami constant K_{Avrami}
2.5	3.15	0.00962	0.22943
5	2.80	0.03558	0.30337
7.5	2.75	0.05819	0.35617
10	2.62	0.09612	0.40861
15	2.25	0.24789	0.53776
20	2.11	0.46314	0.69414

3.9. Polarized Light Microscopy (PLM)

The isothermal crystallization of PEF at temperatures from 190 to 215°C was further studied with PLM. As one can see in the photos of Fig. 11 (a, b), a very large number of small spherulites appeared, even at high crystallization temperatures (210°C). Similar behavior was observed at 215°C. This indicates large nucleation density for PEF. In contrast, PET (Fig. 11 c, d) and PEN (Fig. 11 e, f) can form larger spherulites.

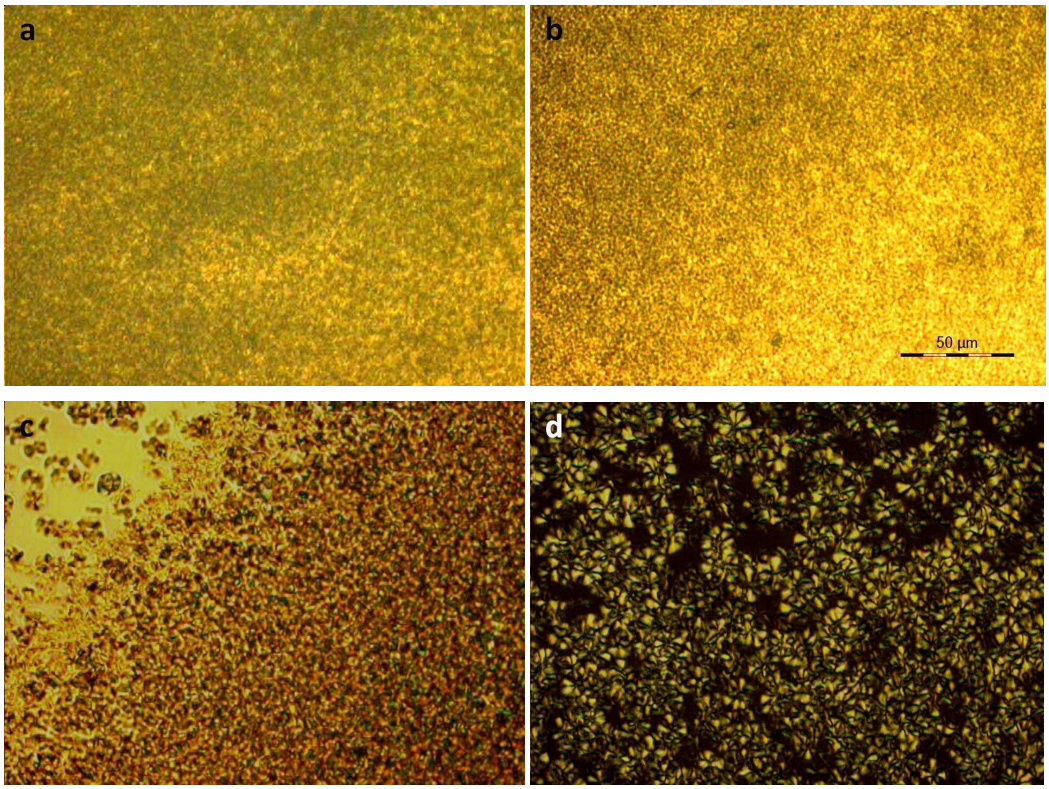

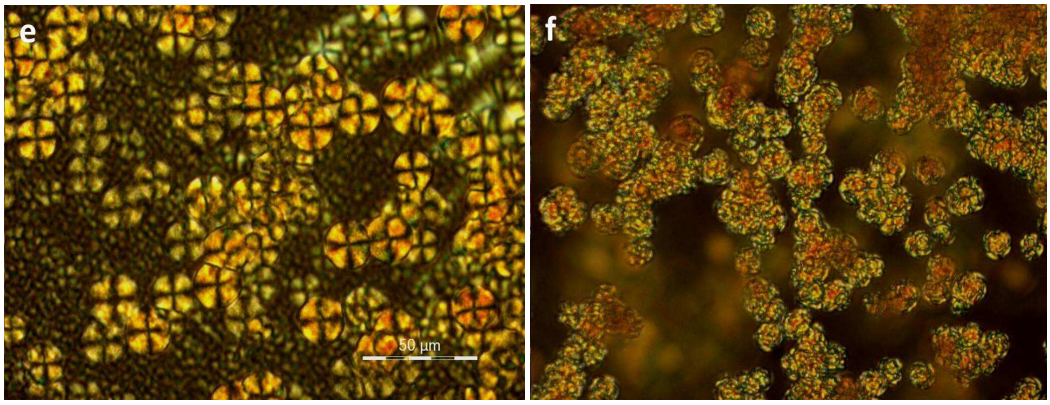

Fig. 11. POM photographs showing morphologies generated on isothermal crystallization: a) PEF at 200°C, b) PEF at 210°C, c) PET 220°C, d) PET 235°C, e) PEN at 190°C, f) PEN at 230°C.

3.10. Thermogravimetric analysis of the polyesters

Thermogravimetric tests on heating at 10°C/min were performed under a nitrogen atmosphere. Fig. 12a shows the remaining mass of the samples as function of temperature. Also, Fig. 12b shows the derivative curve during the tests. It is obvious that thermal degradation of PEF began at lower temperature (about 325°C) than in other polyesters. Degradation of PET started at 340°C, while for PEN at 372°C. However, the temperature at which the maximum degradation rate was achieved was 438°C, 456 and 465°C and the residue at 550 was 13.6 wt%, 20.3 and 36wt% for PEF, PET and PEN respectively. This is obviously associated with the segment corresponding to the carboxylic acid and the ring appearing in the chemical unit of PEF (furanic), PET (benzene) and PEN (naphthalene). In fact even in the synthesis procedure the 2,5-furan-dicarboxylic acid started to degrade at temperatures above 180°C, so the dimethylester of this acid was used since it showed some better stability in the synthesis conditions. The problem was the decarboxylation of the 2,5-furan-dicarboxylic acid. A similar phenomenon, although moderated, is most probably associated with the thermal stability of PEF which seems a little lower than its homologues.

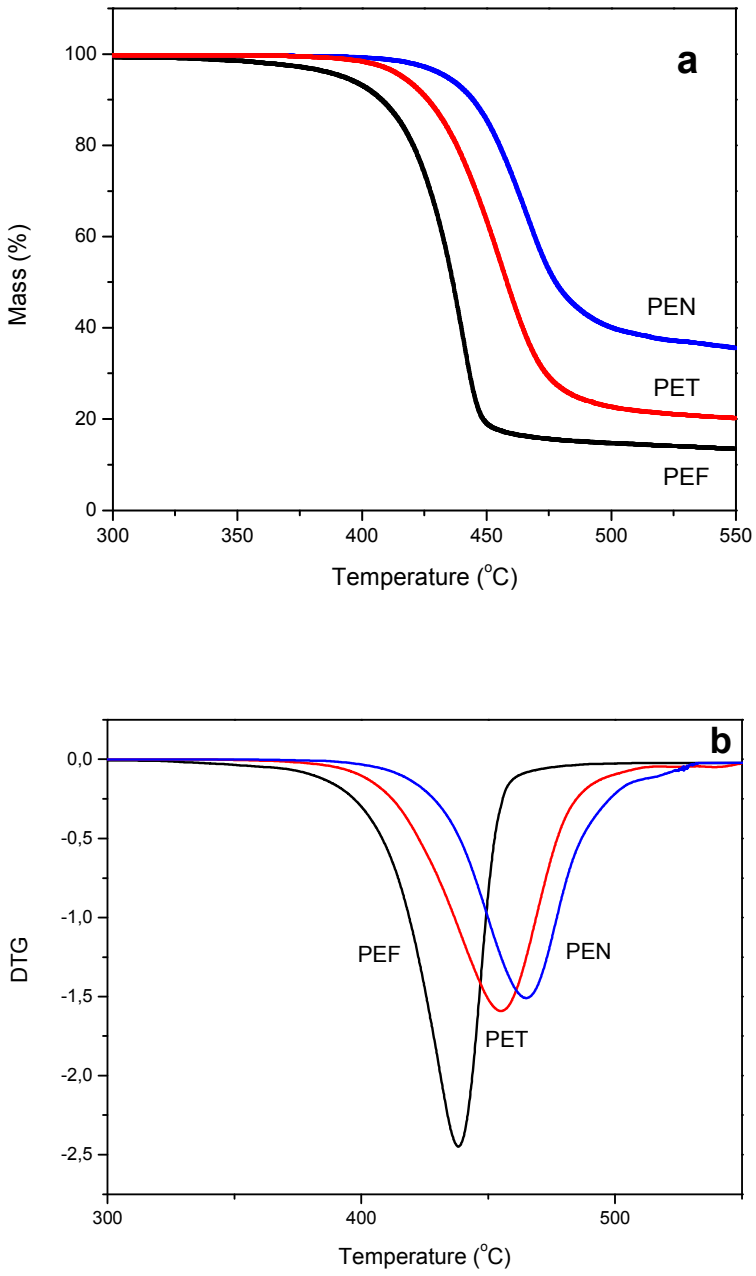

Fig. 12. a) TGA thermogramms and b) derivative TG curves for PEF, PET and PEN, recorded on heating at 10°C/min under Nitrogen atmosphere.

4. Conclusions

The thermal behavior and solid state of PEF were studied with DSC, WAXD and PLM in comparison to PET and PEN. PEF has a T_g of about 87°C, which is higher

than that of PET (80°C), while its apparent melting point is about 217°C. In fact the melting point of samples crystallized at high temperatures can increase to 231°C. The equilibrium melting point of PEF was found 265°C using the ultimate peak temperature. The heat of fusion was estimated to be about 137J/g, which is comparable to that of PET (140J/g), but higher than that of PEN (103J/g). The Avrami exponent (n) values for isothermal crystallization ranged to about 2.2-2.6. The nucleation constant for regime III crystallization was 4.1×10^5, close to that of PET, but lower than that of PEN as was expected because of the differences in the flexibility of the macromolecular chains of the three polymers. From crystallization studies and from T_{cc}-T_g differences it was found that the PEF macromolecular chains are more flexible than those of PEN, but much less flexible than PET ones. PLM observations revealed very small spherulites for PEF and a large nucleation density, even at high crystallization temperatures. Finally, the temperature at which PEF started to decompose was 325°C, about 20°C lower than the respective for PET and about 40°C lower than that of PEN.

References

1 C. Vilela, A.F. Sousa, A.C. Fonseca, A.C. Serra, J.F.J. Coelho, C.S.R. Freire and A.J.D. Silvestre, *Polym. Chem.*, 2014, DOI: 10.1039/C3PY01213A

2 K. Yao, C. Tang, *Macromolecules*, 2013, 46, 1689-1712.

3 D. N. Bikiaris, G.Z. Papageorgiou, D. Giliopoulos, and C. A. Stergiou, *Macrom. Biosci.* 2008, 8, 728–740.

4 G.Z. Papageorgiou and D.N. Bikiaris, *Biomacromolecules,* 2007, 8, 2437-2449.

5 G.Z. Papageorgiou, A.A. Vassiliou, V. D. Karavelidis, A. Koumbis, and D. N. Bikiaris, *Macromolecules*, 2008, 41, 1675-1684.

6 W. Partenheimer, V.V. Grushin, *Adv. Synth. Catal.* 2001, 343, 102-111.

7 J. A. Moore, J. E. Kelly, *Macromolecules,* 1978, 11, 568-573.

8 A. Gandini, A. J. D. Silvestre, C. P. Neto, A. F. Sousa, M. Gomes, *J. Polym. Sci.: Polym. Chem.,* 2009, 47, 295–298.

9 R. J. I. Knoop, W. Vogelzang, J. van Haveren, Daan S. van Es, *J. Polym. Sci.: Polym. Chem.* 2013, 51, 4191–4199.

10 M. Gomes, A. Gandini, A. J. D. Silvestre and B. Reis, *J. Polym. Sci.: Polym. Chem.* 2011, 49, 3759–3768.

11 P. Gopalakrishnan, S. Narayan-Sarathy, T. Ghosh, K. Mahajan and M. N. Belgacem, *J. Polym. Res*., 2014, 21, 340-348.

12 M. Jiang, Q. Liu, Q. Zhang, C. Ye and G. Zhou, *J. Polym. Sci.: Polym. Chem.* 2012, 50, 1026–1036.

13 J. Zhu, J. Cai, W. Xie, P.-H. Chen, M. Gazzano, M. Scandola and R. A. Gross, *Macromolecules,* 2013, 46, 796−804.
14 J. Ma, X. Yu, J. Xu and Yi Pang, *Polymer,* 2012, 53, 4145-4151.
15 E. Gubbels, L. Jasinska-Walc, and C. E. Koning, *J. Polym. Sci.: Polym. Chem.* 2013, 51, 890–898.
16 J. Ma, Y. Pang, M. Wang, J. Xu, H. Mab and X. Nie, *J. Mater. Chem.*, 2012, 22, 3457–3461.
17 A. F. Sousa, M. Matos, C. S. R. Freire, A. J. D. Silvestre and J. F. J. Coelho, *Polymer*, 2013, 54, 513-519.
18 L. Wu, R. Mincheva, Y. Xu, J.-M. Raquez and P. Dubois, *Biomacromolecules,* 2013, 14, 890-899.
19 Z. Yu, J. Zhou, F. Cao, B. Wen, X. Zhu and P. Wei, *J. Appl. Polym. Sci.* 2013, 130, 1415–1420.
20 Y. S. Hu, R. Y. F. Liu, L. Q. Zhang, M. Rogunova, D. A. Schiraldi, S. Nazarenko, Hiltner and E. Baer*, Macromolecules,* 2002, 35, 7326-7337.
21 G. Z. Papageorgiou, D. S. Achilias, G. P. Karayannidis, *Polymer*, 2010, 5, 2565-2575.
22 Tonelli, A., *Polymer*, 2002, 43, 637-642.
23 G. P. Karayannidis, G. Z. Papageorgiou, D. N. Bikiaris and E. V. Tourasanidis, *Polymer* 1998, 39, 4129-4134.
24 B. Fillon, J. C. Wittmann, B. Lotz and A. Thierry, *J. Polym. Sci. Polym. Phys.* 1993, 31, 1383-1393.
25 D. Cavallo, L. Gardella, G. Portale, A. J. Müller and G. C. Alfonso, *Polymer,* 2014, 55, 137-142.
26 S. Vyazovkin , A. K. Burnham , J. M. Criado , L. A. Pérez-Maqueda, C. Popescu, , N. Sbirrazzuoli, *Thermochim. Acta,* 2011, 520, 1-19
27 R. Androsch, B. Wunderlich, *Polymer,* 2005, 46, 12556–12566.
28 S. Z. D. Cheng, B. Wunderlich, *Macromolecules,* 1988, 21, 797-804.
29 B.B. Sauer, W.G. Kampert, E. Neal Blanchard, S.A. Threefoot and B.S. Hsiao, *Polymer,* 2000, *41*, 1099-1108.
30 G.Z. Papageorgiou, G.P. Karayannidis, *Polymer* 1999, *40*, 5325-5332.
31 G. Z. Papageorgiou, D. N. Bikiaris. *Polymer,* 2005, 46, 12081-12092.
32 A. A. Minakov, D. A. Mordvintsev and C. Schick, *Polymer,* 2005, 45, 3755–3763.
33 D. G. Papageorgiou, G. Z. Papageorgiou, E. Zhuravlev, D. Bikiaris, C. Schick and K. Chrissafis, *J. Phys. Chem. B*, 2013, 117, 14875−14884.
34 J. D. Hoffman, J. J. Weeks. *J. Res. Nat. Bur. Stand.-A. Phys. Chem.*, 1961, 66A, 1, 13-28.
35 Z. Chen, J.N. Hay and M.J. Jenkins, *Eur. Polym. J.,* 2013, 49, 2697–2703.
36 X.F. Lu, J.N. Hay, *Polymer,* 2001, 42, 9423-9431.
37 B. Wunderlich, *Pure Appl. Chem.,* 1995, 67, 1019-1026.
38 Avrami, M., *J. Chem. Phys.,* 1939, 7, 1103-1112.
39 D. S. Achilias, G. Z. Papageorgiou and G. P. Karayannidis, *J. Polym. Sci.: Polym. Phys*. 2004, *42*, 3775-3796.

40 G. Z. Papageorgiou, E. Karandrea, D. Giliopoulos, D. G. Papageorgiou, A. Ladavos, A. Katerinopoulou, D. S. Achilias, K. S. Triantafyllidis and D. N. Bikiaris, *Thermochim. Acta,* 2014, 576, 84– 96.
41 J. D. Hoffman, G. T. Davis and Jr. J. I. Lauritzen, *Treatise on solid state chemistry,* N.B. Hannay, Editor. 1976, Plenum: New York. p. 497.
42 S. Vyazovkin, J. Stone, N. Sbirrazzuoli, *J. Thermal Anal. Calorim.,* 2005, 80, 177-180.
43 T. W. Chan, A. I. Isayev. *Polym. Eng. Sci.*, 1994, 34, 461-471.
44 G. Z. Papageorgiou, D. S. Achilias, G. P. Karayannidis, D. N. Bikiaris, C. Roupakias and G. Litsardakis, *Eur. Polym. J.,* 2006, 42, 434–445.
45 Z. Qiu, M. Komura, T. Ikehara and T. Nishi, *Polymer* 2003, 44, 7781–7785.
46 M.L. Di Lorenzo, B. Wunderlich, *Thermochim. Acta,* 2003, 405, 255–268.
47 A. Jeziorny, *Polymer,* 1978, 19, 1142-1149.
48 N. Bosq, N. Guigo, E. Zhuravlev, N. Sbirrazzuoli, *J. Phys. Chem. B* 2013, 117, 3407-3415.

Table of contents

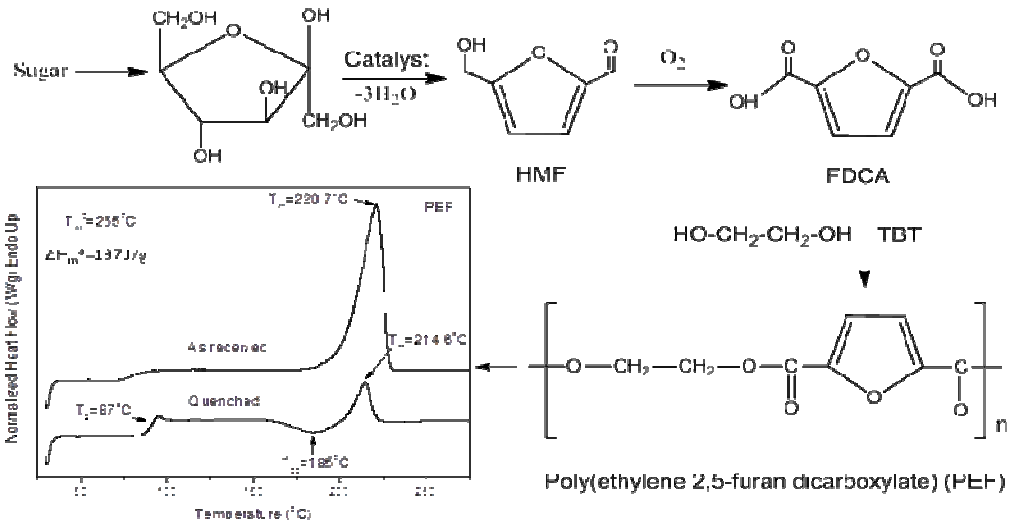

Poly(ethylene-2,5-furan dicarboxylate) (PEF) is a new polyester that can be prepared from monomers derived from renewable resources and its crystallization behavior was studied for first time.